HHS Public Access

Author manuscript

J Chem Phys. Author manuscript; available in PMC 2019 December 10.

Published in final edited form as:

J Chem Phys. 1999 July 1; 111(1): 89–99. doi:10.1063/1.479256.

Definition and properties of the emission anisotropy in the absence of cylindrical symmetry of the emission field: Application to the light quenching experiments

Józef Kuśba[a)], **Joseph R. Lakowicz**

Center for Fluorescence Spectroscopy, Department of Biochemistry and Molecular Biology, University of Maryland at Baltimore, Baltimore, Maryland 21201

Abstract

We considered the properties of the fluorescence anisotropy when the cylindrical symmetry of the fluorescence emission field is absent due to the effects of polarized light quenching. By light quenching we mean stimulated emission by a second longer wavelength pulse following the excitation pulse. In these experiments one observes the excited state population which remains following stimulated emission. When cylindrical symmetry is not present the generally known definition of the emission anisotropy cannot be applied. A generalized theory of anisotropy was described previously by Jabloński. However, we found this formalism to be inadequate for the expected experimental results of light quenching. An extension of this concept, which we call an anisotropy vector, appears capable of describing the expected orientation under all conditions of light quenching. We found that the anisotropy vector can exist within a plane defined by two projections r_H and r_V. The projection r_V is comparable to the classical steady state or time-dependent anisotropy with cylindrical symmetry. The projection r_H has no direct analogue in classical anisotropy theory. The interesting behavior of the anisotropy vector is that all possible points (r_H, r_V) are placed inside a certain triangle, which we call a triangle of anisotropy. For symmetrical molecules, or for molecules which display isotropic depolarizing rotations, the anisotropy vector is expected to decay on the anisotropy triangle along straight lines towards the origin. The concept of the anisotropy vector should allow predictions of the effect of polarized light quenching on the anisotropy decays, and suggests experimental methods to study anisotropy decays in the presence of light quenching. Further work is needed to apply these concepts to anisotropic rotators.

I. INTRODUCTION

To evaluate the fluorescence anisotropy one measures the intensity of the emission through a polarizer. Usually vertically polarized excitation and right-angle observation are chosen (Fig. 1). Then two measurements of the fluorescence intensity, $I_{\parallel}$ and $I_{\perp}$, are carried out with the observation polarizer oriented either parallel (∥) or perpendicular (⊥) to the direction of the electric vector of the polarized excitation. The emission anisotropy is then calculated as[1,2]

[a)]Faculty of Applied Physics and Mathematics. Technical University of Gdańsk, ul. Narutowicza 11/12, 80-952 Gdańsk, Poland.

$$r = \frac{I_{\parallel} - I_{\perp}}{I_{\parallel} + 2I_{\perp}}. \quad (1)$$

The validity of this method of measurement of the emission anisotropy is limited to the cases when the emission field is cylindrically symmetrical, that is, where the value of $I_{\perp}$ remains constant for the observation detector placed anywhere in the $x-y$ plane (Fig. 1). The symmetry properties of the emission field are determined by the symmetry of the observed spatial dependence of the intensity of the luminescence passed through the linear polarizer. In this sense, due to the $\cos^2$ transmission law of the polarizer, the symmetry of the emission field does not always have to be the same as the symmetry of the spatial distribution of the emission transition dipoles. Cylindrical symmetry of the emission field is always observed when an isotropic solution of the fluorophore is excited by a linearly polarized light. Under these conditions one-photon excitation generates values of r belonging to the interval (−0.2, 0.4). Values of r lying outside this interval may be observed when the excitation is a twoor three-photon process.[3] The anisotropy of the fluorescence emission excited by natural or circularly polarized light is also related to two intensity components, $I_{\parallel}$ and $I_{\perp}$. Here the resulting emission field is also cylindrically symmetrical, but the definition of r slightly differs from Eq. (1),

$$r_n = \frac{I_{\parallel} - I_{\perp}}{2I_{\parallel} + I_{\perp}}. \quad (2)$$

The origin of this difference is that for natural or circularly polarized excitation the symmetry axis is not parallel but perpendicular to the electric vector of the excitation light.

Light quenching is a technique which allows modification of the polarized intensity components by stimulated emission.[4–6] In such measurements one observes the remaining fluorescence, not the emission stimulated along the light path of the quenching pulse. In one-pulse light quenching, both excitation and quenching is caused by the same light pulse and the resulting distribution of the emission dipoles is always cylindrically symmetrical. In a two-pulse light quenching experiment the quenching pulse has a different wavelength and is delayed in time. The quenching pulse typically has a longer wavelength to overlap with the emission spectrum of the fluorophore. The quenching pulse is polarized either parallel or perpendicular to the polarization direction of the excitation pulse. In the presence of perpendicular two-pulse light quenching the resulting emission field may not display a cylindrical symmetry.[7,8] For such cases the general definition of r, proposed by Jabloński[9] may be applied

$$r^2 = \frac{\left(I_x - I_y\right)^2 + \left(I_y - I_z\right)^2 + \left(I_z - I_x\right)^2}{2I^2}, \quad (3)$$

where

$$I = I_x + I_y + I_z. \quad (4)$$

In Eq. (3) I_x, I_y, and I_z are the intensities of the emission measured through the observation polarizer oriented parallel to the respective axes of the Cartesian system (Fig. 2). The orientation of the system is selected so that the difference between the strongest and weakest component intensities is maximum. Because the definition (3) does not account for positive or negative values of r, Jabloński suggests that it should be complemented by a convention about the sign. When the sample is excited by a linearly polarized light, two of the intensity components are equal to each other, and Eq. (3) can be written in the form

$$r^2 = \frac{\left(I_{\parallel} - I_{\perp}\right)^2}{\left(I_{\parallel} + 2I_{\perp}\right)^2}. \tag{5}$$

The sign convention used is that r is positive when $I_{\parallel} > I_{\perp}$, and r is negative when $I_{\parallel} < I_{\perp}$. This convention together with Eq. (5) leads to expression (1). Similar considerations allow us to obtain Eq. (2) starting from Eq. (3). The definitions (1)–(3) can be used in both steady-state and time-resolved anisotropy measurements. In time-resolved experiments the intensities I_x, I_y, and I_z or $I_{\parallel}$ and $I_{\perp}$ are understood as dependent on time. These expressions are appropriate when the emission field is symmetrical about the vertical or z-axis. More complex expressions are needed in the absence of cylindrical symmetry.

II. THE ANISOTROPY VECTOR

Assume that intensities I_x, I_y, and I_z are measured within the coordination system oriented so that the difference between the strongest and weakest component intensities is maximum. To understand the meaning of the anisotropy vector we turn our attention to the following identities:

$$I_x = \frac{I}{3}\left(1 + \frac{2I_x - I_y - I_z}{I}\right), \tag{6}$$

$$I_y = \frac{I}{3}\left(1 + \frac{2I_y - I_z - I_x}{I}\right), \tag{7}$$

$$I_z = \frac{I}{3}\left(1 + \frac{2I_z - I_x - I_y}{I}\right). \tag{8}$$

Each of the intensity components can be understood as a sum of the intensity components mean value (I/3) and an additional positive or negative value which describes the anisotropy of the emission field. Let us introduce the following notations:

$$r_x = \frac{1}{\sqrt{6}}\frac{2I_x - I_y - I_z}{I} \equiv \frac{2}{\sqrt{6}I}\left(I_x - \frac{I_y + I_z}{2}\right), \tag{9}$$

$$r_y = \frac{1}{\sqrt{6}}\frac{2I_y - I_z - I_x}{I} \equiv \frac{2}{\sqrt{6}I}\left(I_y - \frac{I_z + I_x}{2}\right), \tag{10}$$

$$r_z = \frac{1}{\sqrt{6}}\frac{2I_z - I_x - I_y}{1} \equiv \frac{2}{\sqrt{6}I}\left(I_z - \frac{I_x + I_y}{2}\right). \tag{11}$$

The quantities r_x, r_y, and r_z describe the relative excess of a given emission component over the average value of the other two emission components, i.e., I_x over $(I_y+I_z)/2$, I_y over $(I_z+I_x)/2$, and I_z over $(I_x+I_y)/2$. These quantities can be understood as the projected magnitudes of a certain vector along the axes of the Cartesian system (r_x, r_y, r_z). We will call this vector a vector of anisotropy $\mathbf{r}$. One can show that the magnitude $|\mathbf{r}|$ of this vector fulfills the following equation:

$$|\mathbf{r}|^2 \equiv r_x^2 + r_y^2 + r_z^2 = \frac{\left(I_x - I_y\right)^2 + \left(I_y - I_z\right)^2 + \left(I_z - I_x\right)^2}{2I^2}. \tag{12}$$

That means that Eq. (3) in fact defines the magnitude of the anisotropy vector. One can also see that

$$r_x + r_y + r_z = 0. \tag{13}$$

Equation (13) means that only two projections of the anisotropy vector are independent. For instance, in the case when r_y and r_z are known one has

$$r^2 = 2\left(r_y^2 + r_y r_z + r_z^2\right). \tag{14}$$

In particular, all three projections of the anisotropy vector are equal to zero if any two of them are equal to zero.

Equation (13) constitutes the equation of a plane in the coordinate system (r_x, r_y, r_z) (Fig. 3). The angle α between this plane (plane of anisotropy) and each of the axes r_x, r_y, and r_z is equal to $\arccos(2/\sqrt{6})$. That means that all anisotropy vectors lie in one plane and that the magnitude and direction of each anisotropy vector can be described by just two numbers. We introduce a new coordinate system (r_H, r_V) with the axes r_H and r_V lying in this plane (Fig. 3) by the transformation

$$r_H = \frac{1}{\sqrt{2}}\left(r_y - r_x\right), \tag{15}$$

$$r_V = \frac{1}{\sqrt{6}}\left(2r_z - r_x - r_y\right). \tag{16}$$

We use the subscript V (vertical) because usually the z-axis is directed vertically in the experiments, and subscript H (horizontal) because the intensities I_x and I_y are detected in the horizontal plane. By substituting Eqs. (9)–(11) for r_x, r_y, r_z in Eqs. (15) and (16) one obtains

$$r_H = \frac{\sqrt{3}}{2}\frac{I_y - I_x}{I}, \tag{17}$$

$$r_V = \frac{2I_z - I_x - I_y}{2I}. \tag{18}$$

The projections r_H and r_V describe the anisotropy of the emission field of any symmetry. Equation (18) may be written in other two forms; $r_V=[I_z-(I_x+I_y)/2]/I$ or $r_V=[(I_z-I_x)+(I_z-I_y)]/(2I)$. This means that the quantity r_V may be understood as describing either the excess of the intensity component I_z over the average value of the intensity components I_x and I_y or the relative mean value of the differences I_z-I_x and I_z-I_y. The quantity r_H describes the relative difference between the intensity components I_x and I_y.

There exists an infinite number of other coordinate systems allowing expression the anisotropy vector as a combination of two components. However, the coordinate system defined by Eqs. (15) and (16) seems to be the most convenient to describe anisotropy of the emission field where the z-axis is a distinguished axis. All possible values of the anisotropy components r_H and r_V are limited by the following three specific points $R=(r_H, r_V)$: $R_x \equiv (-\sqrt{3}/2, -0.5)$, where $I_x=I$ and $I_y=I_z=0$, $R_y \equiv (\sqrt{3}/2, -0.5)$, where $I_y=I$ and $I_x=I_z=0$, and $R_z\equiv(0,1)$, where $I_z=I$ and $I_x=I_y=0$. These three points define an equilateral triangle as shown in Fig. 4. One can show that all other possible points (r_H, r_V) lie on this triangle. The anisotropy values corresponding to the emission fields which are cylindrically symmetrical along the respective axes of the coordinate system (x,y,z), that is describing the cases where $I_x=I_y$, or $I_y=I_z$ or $I_z=I_x$, are placed on the medians of the triangle. In the particular case of z-axis cylindrical symmetry of the emission field $r_H=0$ and the anisotropy is described by magnitude of the projection r_V varying from −0.5 to +1.0. The relative intensities I_x/I, I_y/I, and I_z/I calculated from Eqs. (6)–(8) vary along the respective medians of the triangle from zero to unity (Fig. 5). Points on the R_x, R_y side of the triangle correspond to the class of the emission fields totally polarized in the $x-y$ plane, for which $I_z=0$. Among others, this class involves emission originated from the distribution of the emission dipoles which is rod-like along the x-axis, disc-like in the $x-y$ plane, or rodlike along the y-axis (Fig. 5). Points on the R_x, R_z and R_y, R_z side of the triangle have an analogous interpretation. The centroid of the triangle corresponds to $I_x/I=I_y/I=I_z/I=1/3$ and to the spherically symmetrical emission field. The vertices of the triangle correspond to the emission fields which are rodlike along the respective axes of the coordinate system (x,y,z). If the emission field is a result of excitation by the linearly polarized light and the z-axis is chosen to be parallel to the electric vector of the excitation light then $I_x=I_y$ and Eqs. (17) and (18) simplify to

$$r_H = 0, \quad r_V = \frac{I_\parallel - I_\perp}{I_\parallel + 2I_\perp}. \tag{19}$$

In this case the horizontal component r_H of the anisotropy vanishes and the projection of the anisotropy vector along the r_V-axis is tantamount to the anisotropy defined by Eq. (1) $r=r_V$.

While Eqs. (1) and (3) refers to the same notation (r), the quantities they describe are qualitatively different. Equation (3) describes the magnitude of the anisotropy vector which is always positive and Eq. (1) describes the magnitude of projection of the vector along the r_V-axis, which can be positive, zero, or negative. The comparison of Eqs. (17) and (18) with Eq. (12) implies that the magnitude $|\mathbf{r}|$ of the anisotropy vector is related to r_H and r_V by the equation

$$|\mathbf{r}|^2 = r_H^2 + r_V^2 . \tag{20}$$

The anisotropy defined by Eq. (3) provides only a partial information about the observed symmetry of the emission field. Full information is provided by quantities r_H and r_V defined by Eqs. (17) and (18).

Another interesting interpretation of the anisotropy vector is possible using a Cartesian system with the coordinates representing the relative intensities I_x/I, I_y/I, and I_z/I. In such a system all possible points $(I_x/I, I_y/I, I_z/I)$ lie in the plane $I_x/I+I_y/I+I_z/I=1$. Because none of these intensities can be negative the possible positions of the points $(I_x/I, I_y/I, I_z/I)$ are limited to the triangle with vertices placed in the points (1,0,0), (0,1,0), and (0,0,1) (Fig. 6). One can show that this triangle is tantamount to our triangle of anisotropy. The classical definition of anisotropy (1) can be also discussed in this interpretation by introducing a two-dimensional system $(I_\parallel/I, I_\perp/I)$ (Fig. 6).

To characterize systems for which the emission anisotropy evolves with time one can use the components $r_H(t)$ and $r_V(t)$ of the time-dependent anisotropy vector $r(t)$, defined by the time-dependent forms of Eqs. (17) and (18),

$$r_H(t) = \frac{\sqrt{3}}{2}\frac{I_y(t) - I_x(t)}{I(t)}, \tag{21}$$

$$r_V(t) = \frac{2I_z(t) - I_x(t) - I_y(t)}{2I(t)} . \tag{22}$$

Using r_H and r_V, Eqs. (6)–(8) may be rewritten in the form

$$I_x = \frac{I}{3}\left(1 - r_V - \sqrt{3}r_H\right), \tag{23}$$

$$I_y = \frac{I}{3}\left(1 - r_V + \sqrt{3}r_H\right), \tag{24}$$

$$I_z = \frac{I}{3}\left(1 + 2r_V\right) . \tag{25}$$

The time evolution of the intensity components I_x, I_y, and I_z is described by the time-dependent versions of Eqs. (23)–(25),

$$I_x(t) = \frac{I(t)}{3}\left[1 - r_V(t) - \sqrt{3}r_H(t)\right], \tag{26}$$

$$I_y(t) = \frac{I(t)}{3}\left[1 - r_V(t) + \sqrt{3}r_H(t)\right], \tag{27}$$

$$I_z(t) = \frac{I(t)}{3}\left[1 + 2r_V(t)\right]. \tag{28}$$

Equations (26)–(28) are important for describing the time-dependent polarized intensities in light quenching experiments where the polarization of the quenching pulse is different than that of the excitation pulse. When the quenching light has the same polarization as the excitation light $r_H(t)=0$, $r_V(t)=r(t)$, and one obtains from Eqs. (26)–(28) the well-known equations describing the time evolution of the intensity components of the cylindrically symmetrical emission field

$$I_\perp(t) \equiv I_x(t) = I_y(t) = \frac{I(t)}{3}[1 - r(t)], \tag{29}$$

$$I_\parallel(t) \equiv I_z(t) = \frac{I(t)}{3}[1 + 2r(t)]. \tag{30}$$

If the polarization of the light quenching pulse is not along the same direction as the excitation, then the polarized component decay according to Eqs. (26)–(28). Summarizing this section, one can say that the emission anisotropy can be understood as a vector. The general expression for anisotropy predicted by Jabloński allows calculation of only the magnitude of this vector, but not the values of its components. If the z-axis of the emission field is distinguished then r_H [Eq. (17)] and r_V [Eq. (18)] is a convenient representation of the anisotropy vector. These two quantities completely describe the anisotropy of the emission field of any symmetry. For emission fields displaying cylindrical symmetry along the z-axis, the horizontal projection r_H of the anisotropy vector vanishes and the value of the parallel component r_V becomes equal to the value of r calculated using the classical expression [Eq. (1)]. The time-dependent anisotropy can be described by the time-dependent anisotropy vector $\mathbf{r}(t)$ having two components $r_H(t)$ and $r_V(t)$ defined by Eqs. (21) and (22).

III. CHANGES OF FLUORESCENCE INTENSITY COMPONENTS INDUCED BY LIGHT QUENCHING

We now consider how the anisotropy vector can be used for interpretation of polarized intensity decays under conditions of light quenching. We will consider primarily a two-pulse experiment. The first light pulse excites the sample. The second light pulse, typically at longer wavelengths, causes stimulated emission. This stimulated emission is parallel to the direction of the quenching beam, and is not observed with the usual right angle observation. One observes the emission which has not been quenched.

Light quenching experiments can be performed using polarized excitation, polarized light quenching, and measurement of the polarized emission. If the polarization of the quenching light pulse is parallel to the polarization of the excitation light pulse (parallel quenching) then during the light quenching experiment the vertical projection of the anisotropy vector decreases and the horizontal projection remains equal to zero. The emission field remains cylindrically symmetrical and is described by the two intensity components $I_{\parallel}$ and $I_{\perp}$. The time evolution of these components is given by Eqs. (29) and (30). Assuming that the quenching pulse is short compared to the fluorescence lifetime and rotational diffusion correlation time, both $I(t)$ and $r(t)$ display an instantaneous jump at the quenching pulse arrival time t_d. The intensity jump can be described by the parameter q defined as

$$q = \frac{I_b - I_a}{I_b}, \tag{31}$$

where I_b and I_a are the total fluorescence intensities immediately before and after the quenching pulse. One has to stress that the parameter q describes the jump of the total fluorescence intensity which for parallel quenching is $I=I_{\parallel}+2I_{\perp}$, or $I=I_x+I_y+I_z$ in general. For parallel quenching the jump of the anisotropy can be described by a single parameter Δr defined as

$$\Delta r = r_a - r_b, \tag{32}$$

where r_b and r_a are the fluorescence anisotropies immediately before and after the quenching pulse. This is possible because under the parallel quenching conditions $\Delta r_H=0$ and Δr can be defined as being tantamount to Δr_V.

If the polarization of the quenching light is not parallel to the polarization of the excitation light then both projections of anisotropy vector are affected by the light quenching process. A general description of possible changes of the anisotropy of the emission field may be difficult. In this paper we will discuss only such cases when the emission field before and after the quenching pulse may be described in the same coordinate system (x,y,z). That means we will restrict ourselves to the cases when no rotation of the coordinate system is required to keep the maximum value of the difference between the strongest and weakest intensity component I_x, I_y and I_z of the initial and the light quenching modified emission field. A good example of such case is quenching by light which is polarized perpendicularly with respect to polarization direction of the excitation (perpendicular light quenching). Assume that the z-axis of the coordinate system is directed along the electrical vector of the excitation light and the y-axis along the electrical vector of the quenching light. Under these conditions the time evolution of the intensity components I_x, I_y and I_z is described by Eqs. (26)–(28) with $I(t)$, $r_H(t)$, and $r_V(t)$ displaying instantaneous jumps at $t=t_d$. The jump of the total fluorescence intensity may be described by the parameter q defined by Eq. (31). The jump of the fluorescence anisotropy is related to the anisotropies $\mathbf{r}_b=(r_{bH}, r_{bV})$ and $\mathbf{r}_a=(r_{aH}, r_{aV})$ existing immediately before and after the arrival of the quenching pulse. Because the anisotropy $\mathbf{r}_b$ refers to the cylindrically symmetrical emission field one has $r_{bH}=0$ and $r_{bV}=r_b$, where

$$r_b = \frac{I_{bz} - I_{bx}}{I_{bz} + 2I_{bx}}. \tag{33}$$

In this geometry, light quenching changes the values of all intensity components I_x, I_y, and I_z, but the ratio I_x/I_z remains unaffected (see Appendix A for justification of this property). We assume the rotational diffusion correlation time is long compared to the duration of the quenching pulse, so changes of the spatial distribution of the emission dipoles caused by rotational diffusion during the duration time of the quenching pulse can be neglected. Thus, the anisotropy r_b can be also expressed by the respective intensity components measured immediately after the quenching pulse. Based on Eq. (33) one obtains

$$r_b = \frac{1 - I_{bx}/I_{bz}}{1 + 2I_{bx}/I_{bz}} = \frac{1 - I_{ax}/I_{az}}{1 + 2I_{ax}/I_{az}} = \frac{I_{az} - I_{ax}}{I_{az} + 2I_{ax}}. \tag{34}$$

Taking this into account and applying Eqs. (17) and (18) to the intensity components observed immediately after the quenching pulse one can show that

$$r_{aV} = -\frac{\sqrt{3}}{3}(2r_b + 1)r_{aH} + r_b, \tag{35}$$

This expression indicates that in perpendicular light quenching the possible values of the projections r_H and r_V of the anisotropy vector after the quenching pulse are linearly dependent. One can see that in perpendicular light quenching the horizontally polarized quenching light almost always affects both the horizontal and vertical projections of the anisotropy vector, except the case r_b=−0.5 when only the horizontal projection is modified. All achievable points (r_{aH}, r_{aV}) are placed on the straight lines passing through the lower right corner of the anisotropy triangle and the initial points (0,r_b) (Fig. 7). The limiting vales of the anisotropy $\mathbf{r}_a$ corresponding to very high intensities of the quenching pulse are placed on the R_x, R_z side of the anisotropy triangle and are related to r_b by the equations

$$r_{aH}^{\infty} = \frac{\sqrt{3}}{2}\frac{r_b - 1}{r_b + 2}, \tag{36}$$

$$r_{aV}^{\infty} = \frac{1}{2}\frac{5r_b + 1}{r_b + 2}. \tag{37}$$

The limiting value of the magnitude r_a of the anisotropy vector $\mathbf{r}_a$ is given by

$$r_a^{\infty} = \frac{\left(7r_b^2 + r_b + 1\right)^{1/2}}{r_b + 2}. \tag{38}$$

The change of anisotropy at time t=t_d is characterized by the vector $\Delta\mathbf{r}$=(Δr_H, Δr_V) with the projections Δr_V and Δr_H defined as

$$\Delta r_H = r_{aH} - r_{bH}, \tag{39}$$

$$\Delta r_V = r_{aV} - r_{bV}. \tag{40}$$

Using this notation, the anisotropy of the emission field registered immediately after the quenching pulse may be understood as a sum of two vectors, $\mathbf{r}_b$ and $\Delta\mathbf{r}$,

$$\mathbf{r}_a = \mathbf{r}_b + \Delta\mathbf{r}. \tag{41}$$

In light quenching experiments usually r_{bH}=0 and r_{bV}=r_b, and then Eq. (35) implies that

$$\Delta r_V = -\frac{\sqrt{3}}{3}(2r_b + 1)\Delta r_H. \tag{42}$$

One can see that in the perpendicular light quenching, similarly as in the parallel light quenching, the changes of the intensity components I_x, I_y, and I_z may be described by just two parameters; q and Δr_V or q and Δr_H. We prefer to use q and Δr_H because using Eq. (42) the transformation $\Delta r_V \rightarrow \Delta r_H$ is not possible for r_b=−0.5.

IV. DIFFERENTIAL POLARIZED FLUOROMETRY IN THE CASE OF A CYLINDRICALLY SYMMETRICAL EMISSION FIELD

In differential polarized fluorometry the samples are illuminated with linearly polarized, sinusoidally modulated light with the modulation frequency ω, where ω is in rads. Under these conditions the fluorescence emission field is cylindrically symmetrical and is described by two polarized intensity components $I_\parallel$ and $I_\perp$. Then the phase angle difference Δ_ω between the components and the ratio Λ_ω of the AC signals generated by the two components is measured,[10–12]

$$\Delta_\omega = \varphi_\perp - \varphi_\parallel = \arctan\left(\frac{D_\parallel N_\perp - D_\perp N_\parallel}{D_\parallel D_\perp + N_\parallel N_\perp}\right), \tag{43}$$

$$\Lambda_\omega = \frac{AC_\parallel}{AC_\perp} = \left(\frac{N_\parallel^2 + D_\parallel^2}{N_\perp^2 + D_\perp^2}\right)^{1/2}, \tag{44}$$

where

$$N_k = \int_0^\infty I_k(t)\sin(\omega t)dt, \tag{45}$$

$$D_k = \int_0^\infty I_k(t)\cos(\omega t)dt, \tag{46}$$

and k=∥,⊥. The quantities Δ_ω and Λ_ω depend on the time-zero anisotropy r_0, the modulation frequency ω, and the rate, freedom, and isotropy of fluorophore rotation. Consequently, information about the form of $r(t)$ is available. The meaning of Λ_ω is comparable to that of the intensity ratio of the polarized steady-state intensities. We prefer to present this observable as the modulated anisotropy,[13]

$$r_\omega = \frac{\Lambda_\omega - 1}{\Lambda_\omega + 2}. \tag{47}$$

Equation (47) may be obtained from Eq. (1) by replacing the intensities $I_\parallel$ and $I_\perp$ by the respective AC components, $AC_\parallel$ and $AC_\perp$, of the measured photocurrent and then utilizing Eq. (44). The modulated anisotropy has properties of both the steady-state anisotropy (r) and the fundamental anisotropy (r_0). At modulation frequencies which are low compared to the correlation time, r_ω approaches r. At modulation frequencies much higher than the correlation time, r_ω approaches r_0. The latter property does not fully apply to the light quenching experiments where r_ω may display remarkable oscillations around r_0 at higher modulation frequencies.[6–8]

V. DIFFERENTIAL ANISOTROPY MEASUREMENTS IN THE CASE WHEN THE EMISSION FIELD IS NOT CYLINDRICALLY SYMMETRICAL

If the emission field is not cylindrically symmetrical then, depending on the direction of observation, one can measure three different values for the phase shift ($\Delta_{x\omega}$, $\Delta_{y\omega}$ or $\Delta_{z\omega}$) and three different values for the ratio of the polarized modulated components ($\Lambda_{x\omega}$, $\Lambda_{y\omega}$ or $\Lambda_{z\omega}$),

$$\Delta_{x\omega} = \varphi_y - \varphi_z = \arctan\left(\frac{D_z N_y - D_y N_z}{D_y D_z + N_y N_z}\right), \tag{48}$$

$$\Delta_{y\omega} = \varphi_x - \varphi_z = \arctan\left(\frac{D_z N_x - D_x N_z}{D_x D_z + N_x N_z}\right), \tag{49}$$

$$\Delta_{z\omega} = \varphi_x - \varphi_y = \arctan\left(\frac{D_y N_x - D_x N_y}{D_x D_y + N_x N_y}\right), \tag{50}$$

$$\Lambda_{x\omega} = \frac{AC_z}{AC_y} = \left(\frac{N_z^2 + D_z^2}{N_y^2 + D_y^2}\right)^{1/2}, \tag{51}$$

$$\Lambda_{y\omega} = \frac{AC_z}{AC_x} = \left(\frac{N_z^2 + D_z^2}{N_x^2 + D_x^2}\right)^{1/2}, \tag{52}$$

$$\Lambda_{z\omega} = \frac{AC_y}{AC_x} = \left(\frac{N_y^2 + D_y^2}{N_x^2 + D_x^2}\right)^{1/2}, \tag{53}$$

where N_k and D_k are given by Eqs. (45) and (46) with $k = x,y,z$. From the above six quantities only four are independent, e.g., $\Delta_{x\omega}$ is related to $\Delta_{y\omega}$ and $\Delta_{z\omega}$, and $\Lambda_{x\omega}$ is related to $\Lambda_{y\omega}$ and $\Lambda_{z\omega}$,

$$\Delta_{x\omega} = \Delta_{y\omega} - \Delta_{z\omega}, \quad \Lambda_{x\omega} = \frac{\Lambda_{y\omega}}{\Lambda_{z\omega}}. \tag{54}$$

It seems that the most convenient way to measure the anisotropy of the emission field which does not display the cylindrical symmetry is to use the right angle observation and measure $\Delta_{y\omega}$ and $\Lambda_{y\omega}$ with vertical orientation of the excitation polarizer. One can then rotate the excitation polarizer to the horizontal orientation, and measure $\Delta_{z\omega}$ and $\Lambda_{z\omega}$ (Fig. 8). These data can then be fit using appropriate models for intensity and anisotropy decay. The quantities $\Lambda_{y\omega}$ and $\Lambda_{z\omega}$ may be presented as the modulated horizontal anisotropy

$$r_{H\omega} = \frac{\sqrt{3}}{2}\frac{\Lambda_{z\omega} - 1}{\Lambda_{y\omega} + \Lambda_{z\omega} + 1}, \tag{55}$$

and/or modulated vertical anisotropy

$$r_{V\omega} = \frac{2\Lambda_{y\omega} - \Lambda_{z\omega} - 1}{2\left(\Lambda_{y\omega} + \Lambda_{z\omega} + 1\right)}. \tag{56}$$

Equations (55) and (56) may be obtained on the way analogous to that applied to obtain Eq. (47), using Eqs. (17), (18), (52), and (53). In the cylindrically symmetrical limit of Eqs. (48)–(53) one obtains $\Delta_{x\omega}=\Delta_{y\omega}=\Delta_{\omega}$, $\Delta_{z\omega}=0$, $\Lambda_{x\omega}=\Lambda_{y\omega}=\Lambda_{\omega}$, and $\Lambda_{z\omega}=1$, yielding $r_{H\omega}=0$ and $r_{V\omega}=r_{\omega}$ [Eq. (47)]. Similar to r_{ω}, the modulated vertical anisotropy and the modulated horizontal anisotropy become at low modulation frequencies the steady-state anisotropies r_H and r_V, respectively, and at high modulation frequencies much higher then the correlation time—the time-zero anisotropies r_{H0} and r_{V0}, respectively. In the light quenching experiments at high modulation frequencies $r_{H\omega}$ and $r_{V\omega}$ display oscillations around r_{H0} and r_{V0}, respectively.

VI. INFLUENCE OF LIGHT QUENCHING AND ROTATIONAL DIFFUSION ON THE ANISOTROPY DECAY

In liquid solvents the luminescent molecules perform Brownian rotations due to the thermal motion. This phenomenon causes the relative Contributions of $I_x(t)$, $I_y(t)$, and $I_z(t)$ to the total intensity $I(t)$ to change with time. If the molecules may be treated as nonhindered rotators the result of the Brownian rotations is that the differences between $I_x(t)$, $I_y(t)$, and $I_z(t)$ relative to the total intensity $I(t)$ tend to zero. However, the total intensity $I(t)=I_x(t)+I_y(t)$

$+I_Z(t)$ remains independent of the molecular rotation. In the presence of one-pulse or two-pulse light quenching the fluorescence intensity decay takes the form

$$I(t) = \begin{cases} I^0(t) & \text{for } 0 \leqslant t \leqslant t_d, \\ (1-q)I^0(t) & \text{for } t > t_d, \end{cases} \tag{57}$$

where q is defined by Eq. (31), τ is the mean decay time, and t_d denotes the time delay of the quenching pulse, and $I^0(t)$ the intensity decay in the absence of the light quenching pulse. It is assumed that the total fluorescence decay before and after the quenching pulse is described by the same time-dependent function. This may be not applicable in the case of mixtures of fluorescent fluorophores when each fluorophore in the mixture is quenched to a different extent. The explicit expression for the function $I^0(t)$, characterizing the luminescence intensity in the absence of light quenching, depends on the particular system under investigation. It can be represented by a single exponential, multiexponential, or any other function. Note that the appropriate forms of equations describing the one-pulse light quenching experiments may be obtained by setting t_d=0 in the equations describing the two-pulse experiments. The effect of Brownian rotations on the fluorescence anisotropy depends on the symmetry of the luminescent molecules, and the kind and efficiency of the light quenching. A general theoretical description of these phenomena may easily become very complicated. In the following subsections we discuss the influence of light quenching on the emission anisotropy in the simplest cases, i.e., when the fluorescence emission is excited by the linearly polarized light. In these cases the emission field in the absence of light quenching remains cylindrically symmetrical for all times shorter then the time of arrival of the quenching pulse. The discussion will be also limited to the simple light quenching experiments when the quenching pulse is polarized either parallel or perpendicular to the polarization direction of the excitation pulse.

A. Spherical molecules

It has been shown by Perrin[14–16] that for spherical molecules the emission anisotropy $r(t)$ of the cylindrically symmetrical emission field decays exponentially with time

$$r(t) = r_0 e^{-t/\Theta}, \tag{58}$$

where r_0 is the fluorescence anisotropy at t=0 and Θ is the rotational diffusion correlation time. Using the same formalism one can show (see Appendix B) that for spherical molecules generating a noncylindrically symmetrical emission field, the projections $r_H(t)$ and $r_V(t)$ also decay exponentially,

$$r_H(t) = r_{H0} e^{-t/\Theta}, \tag{59}$$

$$r_V(t) = r_{V0} e^{-t/\Theta}. \tag{60}$$

Equations (59) and (60) involve the same time-dependent term $\exp(-t/\Theta)$. This implies that in this case, due to rotational diffusion, the anisotropy evolves from the arbitrary starting

point (r_{H0}, r_{V0}) towards the origin along the straight line. For the case of excitation by the linearly polarized light, accompanied (t_d=0) or followed (t_d>0) by the light quenching Eqs. (59) and (60) take the form

$$r_H(t) = \begin{cases} 0 & \text{for } 0 \leqslant t \leqslant t_d, \\ r_{aH} e^{-(t-t_d)/\Theta} & \text{for } t > t_d, \end{cases} \tag{61}$$

$$r_V(t) = \begin{cases} r_0 e^{-t/\Theta} & \text{for } 0 \leqslant t \leqslant t_d \\ r_{aV} e^{-(t-t_d)/\Theta} & \text{for } t > t_d, \end{cases} \tag{62}$$

where

$$r_{aV} = r_0 e^{-t_d/\Theta} + \Delta r_V, \tag{63}$$

or taking into account Eq. (42),

$$r_{aV} = r_0 e^{-t_d/\Theta} - \frac{\sqrt{3}}{3}\left(2 r_0 e^{-t_d/\Theta} + 1\right)\Delta r_H, \tag{64}$$

and

$$r_{aH} = \Delta r_H . \tag{65}$$

After substituting Eqs. (57), (61), and (62) for $I(t)$, $r_H(t)$, and $r_V(t)$ in Eqs. (26)–(28) one obtains

$$I_x(t) = \begin{cases} \frac{1}{3} I^0(t)\left[1 - r_0 e^{-t/\Theta}\right] & \text{for } 0 \leqslant t \leqslant t_d, \\ \frac{1}{3}(1-q) I^0(t)\left[1 - \left(r_{aV} + \sqrt{3} r_{aH}\right) e^{-(t-t_d)/\Theta}\right] & \text{for } t > t_d, \end{cases} \tag{66}$$

$$I_y(t) = \begin{cases} \frac{1}{3} I^0(t)\left[1 - r_0 e^{-t/\Theta}\right] & \text{for } 0 \leqslant t \leqslant t_d, \\ \frac{1}{3}(1-q) I^0(t)\left[1 - \left(r_{aV} - \sqrt{3} r_{aH}\right) e^{-(t-t_d)/\Theta}\right] & \text{for } t > t_d, \end{cases} \tag{67}$$

$$I_z(t) = \begin{cases} \frac{1}{3} I^0(t)\left[1 + 2 r_0 e^{-t/\Theta}\right] & \text{for } 0 \leqslant t \leqslant t_d, \\ \frac{1}{3}(1-q) I^0(t)\left[1 + 2 r_{aV} e^{-(t-t_d)/\Theta}\right] & \text{for } t > t_d . \end{cases} \tag{68}$$

The above expressions can be used for calculation of the phase shifts $\Delta_{k\omega}$ and ratios $\Lambda_{k\omega}$ given by Eqs. (48)–(53). After that, by comparison of the calculated values of $\Delta_{k\omega}$ and $\Lambda_{k\omega}$

with those found experimentally, the unknown light quenching parameters q and Δr_H can be evaluated. The parameter Δr_V can be evaluated later from Eq. (38). One has to notice that in general, the parameters q, Δr_H, and Δr_V are highly correlated and may be expressed by a single parameter describing the number of photons passing the light quenching cross section of the molecule during a single quenching pulse. This problem will be treated in more detail in a future paper.

For the parallel light quenching, the emission field remains cylindrically symmetrical for all times, and then Eqs. (66)–(68) simplify to

$$I_{\parallel}(t) = \begin{cases} \frac{1}{3} I^0(t)\left[1 + 2r_0 e^{-t/\Theta}\right] & \text{for } 0 \leqslant t \leqslant t_d, \\ \frac{1}{3}(1-q) I^0(t)\left[1 + 2r_a e^{-\left(t - t_d\right)/\Theta}\right] & \text{for } t > t_d, \end{cases} \tag{69}$$

$$I_{\perp}(t) = \begin{cases} \frac{1}{3} I^0(t)\left[1 - r_0 e^{-t/\Theta}\right] & \text{for } 0 \leqslant t \leqslant t_d, \\ \frac{1}{3}(1-q) I^0(t)\left[1 - r_a e^{-\left(t - t_d\right)/\Theta}\right] & \text{for } t > t_d, \end{cases} \tag{70}$$

where

$$r_a = r_0 e^{-t_d/\Theta} + \Delta r\,. \tag{71}$$

In this case, the number of unknown light quenching parameters is reduced to two, q and Δr, defined by Eqs. (31) and (32).

B. Nonspherical molecules under one-beam or two-beam parallel light quenching

In this case the emission field remains cylindrically symmetrical for the entire fluorescence decay. The z-axis of the coordinate system can be chosen parallel to the symmetry axis of the emission field. Under these conditions the horizontal projection of the anisotropy vector remains equal to zero and the emission anisotropy is fully described by the vertical projection $r_V(t)=r(t)$. It has been shown that for nonspherical molecules excited by the linearly polarized light the emission anisotropy decays as a sum of exponentials,[17–19]

$$r(t) = r_0 \sum_{j=1}^{n} g_j e^{-t/\Theta_j}, \tag{72}$$

where the correlation times Θ_j are expressed by combinations of components of the diffusion tensor, and the amplitudes g_j are dependent on the wave functions of the asymmetric rotor, the initial angular distribution of the transition dipoles and the properties of the observation polarizer. The number n of different correlation times may not exceed five. One can expect that light quenching will not change the correlation times Θ_j, which are determined by the diffusion tensor. However, light quenching can be expected to change the amplitudes g_j as a result of modification of the spatial distribution of the transition dipoles. Thus, in the

presence of the parallel light quenching the anisotropy decay of nonspherical molecules can be described by the equation

$$r(t) = \begin{cases} r_0 \sum_{j=1}^{n} g_j e^{-t/\Theta_j} & \text{for } 0 \leqslant t \leqslant t_d, \\ r_a \sum_{j=1}^{n} g_j^{l} e^{-(t-t_d)/\Theta_j} & \text{for } t > t_d, \end{cases} \tag{73}$$

where g'_j are the new, light quenching modified amplitudes associated with the particular correlation times Θ_p and r_a is given by

$$r_a = r_0 \sum_{g_j} e^{-t_d/\Theta_j} + \Delta r\,. \tag{74}$$

Due to possible changes of amplitudes g_j, one can anticipate a possibility that certain correlation times which are difficult to retrieve from the classical measurements may become experimentally measurable after the act of light quenching. As for spherical molecules, the anisotropy of the emission field generated by the nonspherical molecules and modified by the process of parallel light quenching also evolves on the anisotropy triangle along the straight line. This line is described by the equation r_H=0. To find the expressions for the parallel and perpendicular components of the intensity decay one has to substitute Eq. (57) for $I(t)$ and Eq. (73) for $r(t)$ in Eqs. (29) and (30). These expressions may then be used to calculate the frequency-domain observables, the phase difference Δ_ω and the ratio Λ_ω based on Eqs. (43) and (44), respectively.

C. Nonspherical molecules under two-beam perpendicular light quenching

In this case the emission field will lose cylindrical symmetry after the quenching pulse, and then both projections $r_H(t)$ and $r_V(t)$ of the anisotropy vector will decay heterogeneously. At present we do not know if the decays of these projections will be described by one common time-dependent function or by two different functions. The additional calculations to solve this problem are not within the scope of this paper. Assuming two different time dependencies for $r_H(t)$ and $r_V(t)$ one can write

$$r_H(t) = \begin{cases} 0 & \text{for } 0 \leqslant t \leqslant t_d, \\ r_{aH} \sum_{j=1}^{n} g_{Hj} e^{-(t-t_d)/\Theta_j} & \text{for } t > t_d, \end{cases} \tag{75}$$

$$r_V(t) = \begin{cases} r_0 \sum_{j=1}^{n} g_j e^{-t/\Theta_j} & \text{for } 0 \leqslant t \leqslant t_d, \\ r_{aV} \sum_{j=1}^{n} g_{Vj} e^{-(t-t_d)/\Theta_j} & \text{for } t > t_d, \end{cases} \tag{76}$$

where

$$r_{aV} = r_0 \sum_{j=1}^{n} g_j e^{-t_d/\theta_j} + \Delta r_V \quad (77)$$

and r_{aH} is given by Eq. (65). In this case after the quenching pulse the emission anisotropy would not evolve towards the origin along the straight line on the anisotropy triangle. In order to find the intensity decays $I_x(t)$, $I_y(t)$, and $I_z(t)$ one should substitute expressions (57) and (75)–(77) for $I(t)$, $r_H(t)$, and $r_V(t)$ in Eqs. (26)–(28). Using these new decay functions and Eqs. (48)–(53) one can theoretically predict the phase shifts $\Delta_{k\omega}$ and amplitude ratios $\Lambda_{k\omega}$. Comparison of the calculated values of $\Delta_{k\omega}$ and $\Lambda_{k\omega}$ may allow determination of the anisotropy changes Δr_H and Δr_V, and the light quenching modified amplitude factors g_{Hj} and g_{Vj}.

VII. CONCLUSIONS

The phenomenon of light quenching may generate emission fields which do not display cylindrical symmetry. For such fields the generally known definition of the emission anisotropy is not adequate. A new concept called an anisotropy vector is capable of describing the existing state of the emission field of any symmetry. The anisotropy vector is defined in the Cartesian system (r_x, r_y, r_z) and cannot be shown in the laboratory system (x,y,z). The possible orientations of the anisotropy vector are limited to the plane defined by the equation $r_x+r_y+r_z=0$ which allows for full description of the vector by just two components. In this plane we found a new system (r_H, r_V) in which the projection r_V of the anisotropy vector corresponds to the classical definition of anisotropy with cylindrical symmetry. The relations of the projections r_H and r_V to the polarized intensity components I_x, I_y, and I_z are given by Eqs. (17) and (18). The projection r_H has no analog in the classical anisotropy theory. All possible points (r_H, r_V) are placed inside an equilateral triangle, which we call the triangle of anisotropy. In the usual anisotropy experiments the horizontal projection, r_H, is usually equal to zero. States with a nonzero horizontal projection of the anisotropy vector can be achieved after the act of the perpendicular light quenching. In this case the possible changes of both projections are fully correlated [Eqs. (35) and (42)]. For freely rotating fluorescent molecules, the anisotropy vector tends with time to zero. If the molecules are spherical or display isotropic rotations then, due to rotational diffusion, the anisotropy evolves from any starting point (r_H, r_V) towards the origin along the straight line. This may not be true for emission fields generated by molecules displaying anisotropic rotations when emission is modified by the perpendicular light quenching. One can expect that for heterogenous anisotropy decay, light quenching may change values of the preexponential factors associated with the observed correlation times.

APPENDIX A

Using the coordinate system shown in Fig. 9, the time dependent intensity components $I_x(t)$ and $I_z(t)$ can be expressed as

$$I_x(t) = c_1 \int_0^{2\pi} \int_0^{\pi/2} n(\alpha, \beta, t) \sin^3 \alpha \sin^2 \beta \, d\alpha \, d\beta, \tag{A1}$$

$$I_z(t) = c_1 \int_0^{2\pi} \int_0^{\pi/2} n(\alpha, \beta, t) \sin^3 \alpha \cos^2 \beta \, d\alpha \, d\beta, \tag{A2}$$

where c_1 is a constant, and $n(\alpha,\beta,t)$ is the angular distribution of the transition moments of the excited molecules at time t. If the electrical vector of the quenching pulse is directed along the y-axis then based on Eq. (44) from Ref. 8 the distribution $n(\alpha,\beta,t)$ is given by

$$n(\alpha, \beta, t) = \begin{cases} n_0(\alpha, \beta) e^{-t/\tau}, & \text{for } 0 \leqslant t \leqslant t_d, \\ n_0(\alpha, \beta) e^{-S_{p2} \cos^2 \alpha} e^{-1/\tau}, & \text{for } t > t_d, \end{cases} \tag{A3}$$

where $n_0(\alpha,\beta)$ is angular distribution of the transition moments of the excited molecules at time t=0 and S_{p2} is a certain parameter proportional to the quenching power. One can see from Eq. (A3) that the distribution $n_a(\alpha,\beta,t_d)$ observed immediately after the quenching pulse is related to the distribution $n_b(\alpha,\beta,t_d)$ observed immediately before the quenching pulse by the equation

$$n_a(\alpha, \beta, t_d) = n_b(\alpha, \beta, t_d) e^{-S_{p2} \cos^2 \alpha}. \tag{A4}$$

Equations (A3) and (A4) are strictly valid for modest extents of light-quenching and high levels of quenching. The distribution of depleted fluorophore will be proportional to $\cos^2\alpha$, and a somewhat broader distribution will be depleted with larger extents of light-quenching.

Using Eq. (A4) one can rewrite Eqs. (A1) and (A2) in the form

$$I_{bx} = c_1 \int_0^{2\pi} \sin^2 \beta \int_0^{\pi/2} n_b(\alpha, \beta, t_d) \sin^3 \alpha d\alpha \, d\beta, \tag{A5}$$

$$I_{bz} = c_1 \int_0^{2\pi} \cos^2 \beta \int_0^{\pi/2} n_b(\alpha, \beta, t_d) \sin^3 \alpha d\alpha \, d\beta, \tag{A6}$$

$$I_{ax} = c_1 \int_0^{2\pi} \sin^2 \beta \int_0^{\pi/2} n_b(\alpha, \beta, t_d) \times \exp\left(-S_{p2} \cos^2 \alpha\right) \sin^3 \alpha \, d\alpha \, d\beta, \tag{A7}$$

$$I_{az} = c_1 \int_0^{2\pi} \cos^2 \beta \int_0^{\pi/2} n_b(\alpha, \beta, t_d) \times \exp\left(-S_{p2} \cos^2 \alpha\right) \sin^3 \alpha \, d\alpha \, d\beta \, . \tag{A8}$$

Because the integrals over alpha within the pairs I_{bx}, I_{bz} and I_{ax}, I_{az} are equal to each other, one obtains $I_{bx}/I_{bz}=I_{ax}/I_{az}$, independently on the shape of distribution $n_b(\alpha,\beta,t_d)$ observed immediately before the quenching pulse.

APPENDIX B

The time dependence of the emission anisotropy of Brownian molecules is a function of their orientation. This orientation may be described by nine direction cosines $C_{ij}=\cos(i,j)$, ($i=x,y,z$; $j=X,Y,Z$). The direction cosines determine the actual position of the coordinate axes (x,y,z) of the Cartesian system fixed to the molecule, relative to the initial position of these axes (X,Y,Z). It has been shown previously[14–16,20] that during the isotropic Brownian motion the mean values of the direction cosines fulfill the relation $\langle C_{xX}^2\rangle=\langle C_{yY}^2\rangle=\langle C_{zZ}^2\rangle$ and $\langle C_{ij}^2\rangle=\langle C_{ik}^2\rangle$. Besides, for spherical molecules one obtains

$$\langle C_{ii}\rangle=\frac{1}{3}\left(1+2e^{-t/\Theta}\right), \tag{B1}$$

$$\langle C_{ij}\rangle=\frac{1}{3}\left(1-e^{-t/\Theta}\right), \tag{B2}$$

where Θ is the rotational diffusion correlation time. The time evolution of the intensity components $I_x(t)$, $I_y(t)$, and $I_z(t)$ may be written in the form

$$I_k(t)=\alpha(t)\left[I_{X0}\langle C_{xk}^2\rangle+I_{\gamma 0}\langle C_{yk}^2\rangle+I_{Z0}\langle C_{zk}^2\rangle\right], \tag{B3}$$

where I_{X0}, I_{Y0}, and I_{Z0} are the initial values of these components related to the total initial luminescence intensity I_0 by the equation

$$I_0=I_{X0}+I_{Y0}+I_{Z0}. \tag{B4}$$

The function $\alpha(t)$ describes the decay of the I_0,

$$I(t)=I_0\alpha(t). \tag{B5}$$

Using Eqs. (B3) and (B1)–(B2) one can show that for spherical molecules any difference of the intensity components decays according to the relation

$$I_i(t)-I_j(t)=\alpha(t)\left(I_{i0}-I_{j0}\right)e^{-t/\Theta}. \tag{B6}$$

The anisotropies $r_H(t)$ and $r_V(t)$ [(Eqs. (21) and (22)] can be represented by linear combinations of such differences [see also discussion following Eqs. (17) and (18)]. After utilizing Eqs. (B5) and (B6), and introducing denotations

$$r_{V0}=\frac{2I_{Z0}-I_{X0}-I_{Z0}}{2I_0}, \tag{B7}$$

$$r_{H0} = \frac{\sqrt{3}}{2}\frac{I_{Y0} - I_{X0}}{I_0}, \tag{B8}$$

one obtains Eqs. (59) and (60).

References

1. Jabłoński A, Acta Phys. Pol 26, 471 (1957).
2. Jabłoński A, Bull. Acad. Pol. Sci., Ser. Sci., Math., Astron. Phys 8, 259 (1960).
3. Topics in Fluorescence Spectroscopy, edited by Lakowicz JR (Plenum, New York, 1997), Vol. 5, p. 544.
4. Mazurenko YT, Opt. Spectrosc 35, 137 (1973).
5. Gryczynski I, Bogdanov V, and Lakowicz JR, J. Fluoresc 3, 85 (1993). [PubMed: 24234772]
6. Gryczynski I, Kuśba J, and Lakowicz JR, J. Phys. Chem 98, 8886 (1994).
7. Lakowicz JR, Gryczynski I, and Kuśba J, Photochem. Photobiol 60, 546 (1994). [PubMed: 7870760]
8. Kuśba J, Bogdanov V, Gryczynski I, and Lakowicz JR, Biophys. J 67, 2024 (1994). [PubMed: 7858140]
9. Jabłoński A, Postepy Fiz. 18, 663 (1967).
10. Weber G, J. Chem. Phys 66, 4081 (1977).
11. Mantulin WW and Weber G, J. Chem. Phys 66, 4092 (1997).
12. Lakowicz JR, Cherek H, Kuśba J, Gryczynski I, and Johnson ML, J. Fluoresc 3, 103 (1993). [PubMed: 24234774]
13. Maliwal BP and Lakowicz JR, Biochim. Biophys. Acta 873, 173 (1986). [PubMed: 3756174]
14. Perrin F, Ann. Phys 12, 169 (1929).
15. Perrin F, Hebd CR. Seances Acad. Sci 181, 414 (1925).
16. Perrin F, J. Phys 7, 390 (1926).
17. Chuang TJ and Eisenthal KB, J. Chem. Phys 57, 5094 (1972).
18. Ehrenberg M and Rigler R, Chem. Phys. Lett 14, 539 (1972).
19. Belford GG, Belford RL, and Weber G, Proc. Natl. Acad. Sci. USA 69, 1392 (1972). [PubMed: 4504348]
20. Kawski A, Crit. Rev. Anal. Chem 23, 459 (1993).

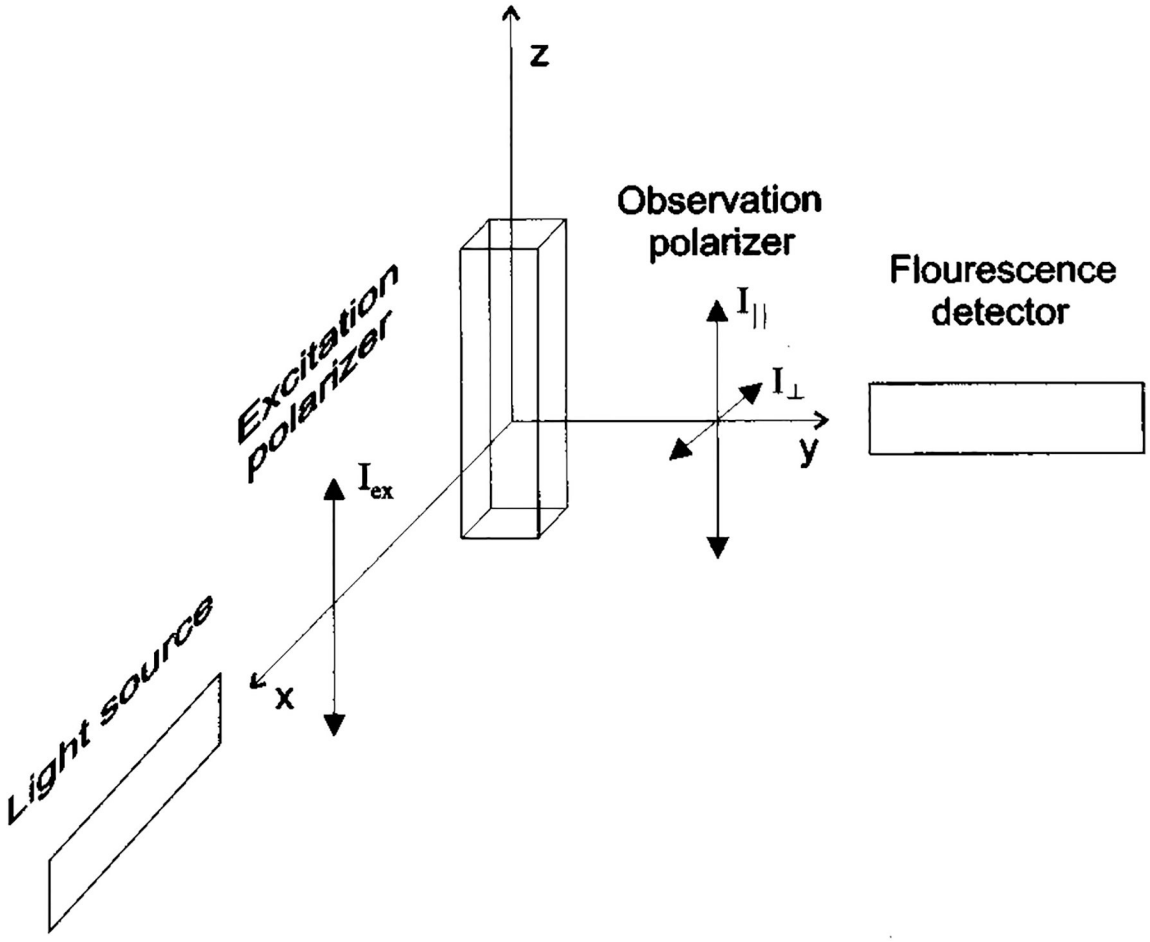

FIG. 1.

Schematic diagram for measurement of fluorescence anisotropy of a cylindrically symmetrical emission field.

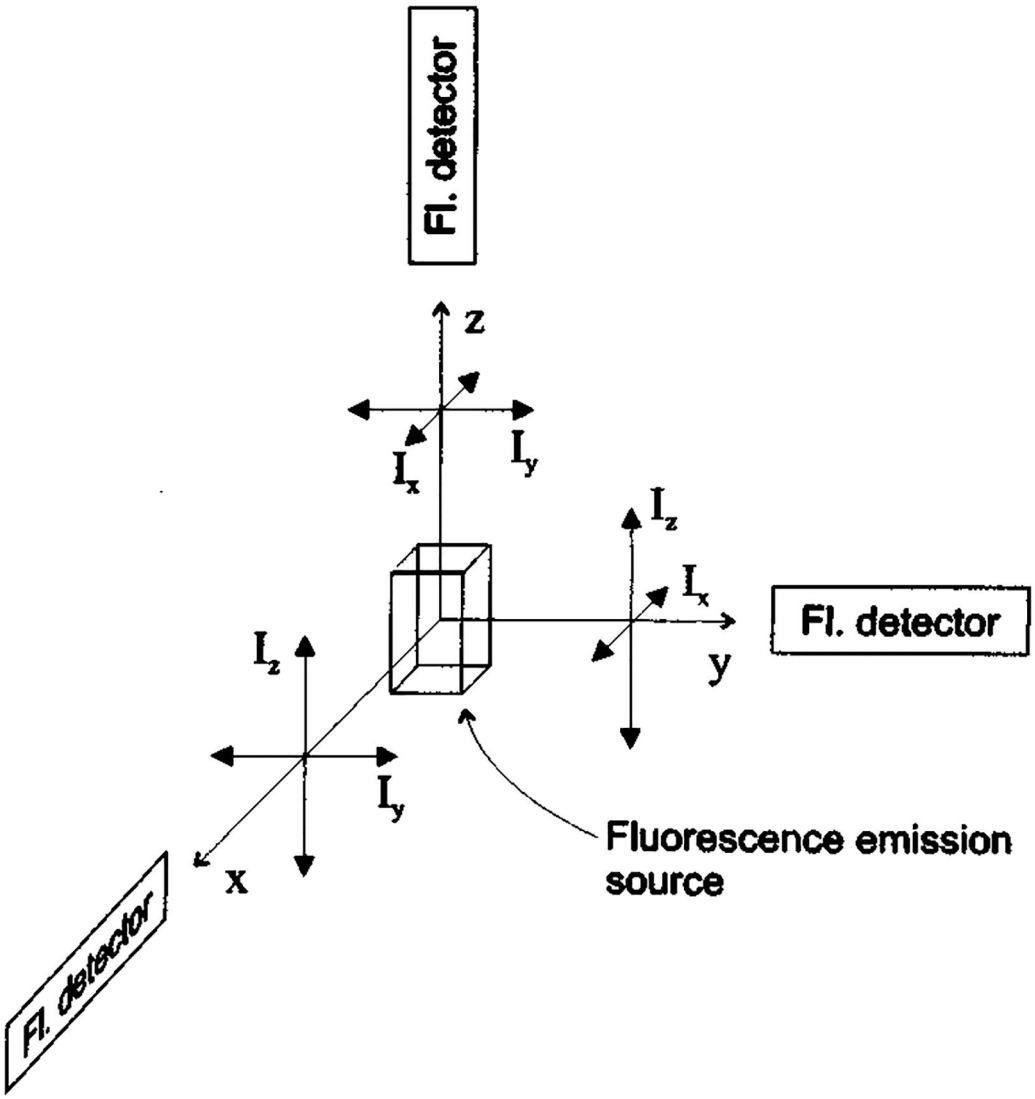

FIG. 2.

Schematic diagram for measurement of the polarized intensities I_x, I_y, I_z of an emission field of arbitrary symmetry. The orientation of the Cartesian system (x,y,z) should be selected so that the difference between the strongest and weakest component intensities is maximum.

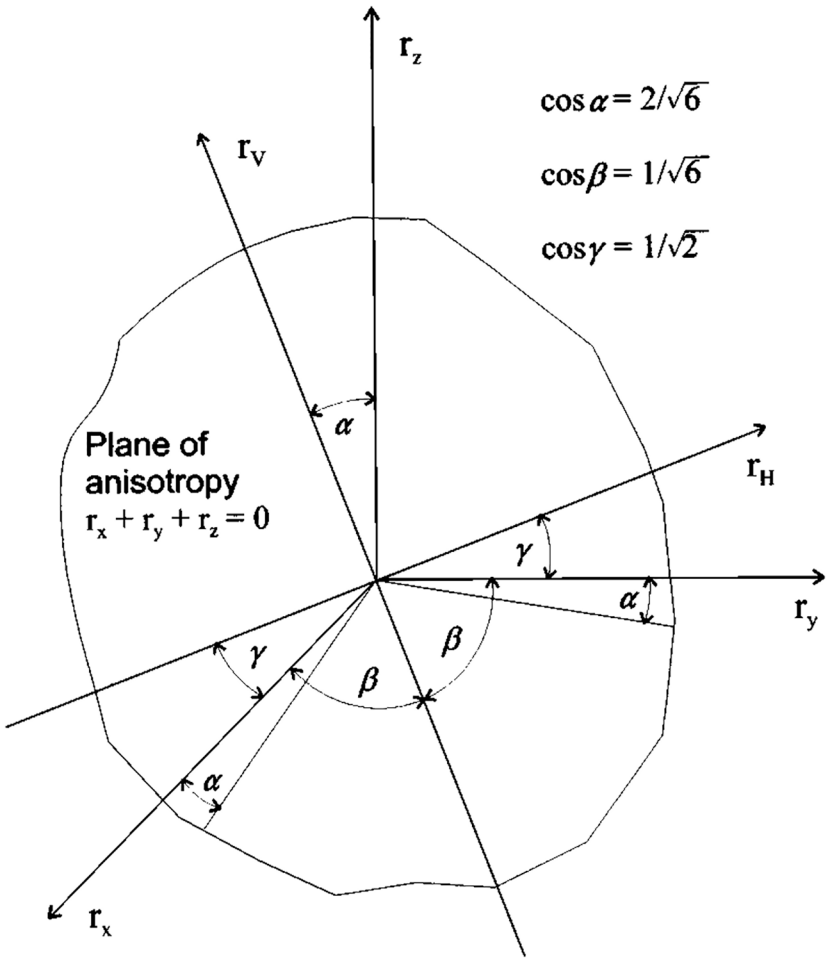

FIG. 3.

Orientation of the plane of anisotropy and coordinate system (r_H, r_V) in the coordinate system (r_X, r_Y, r_Z).

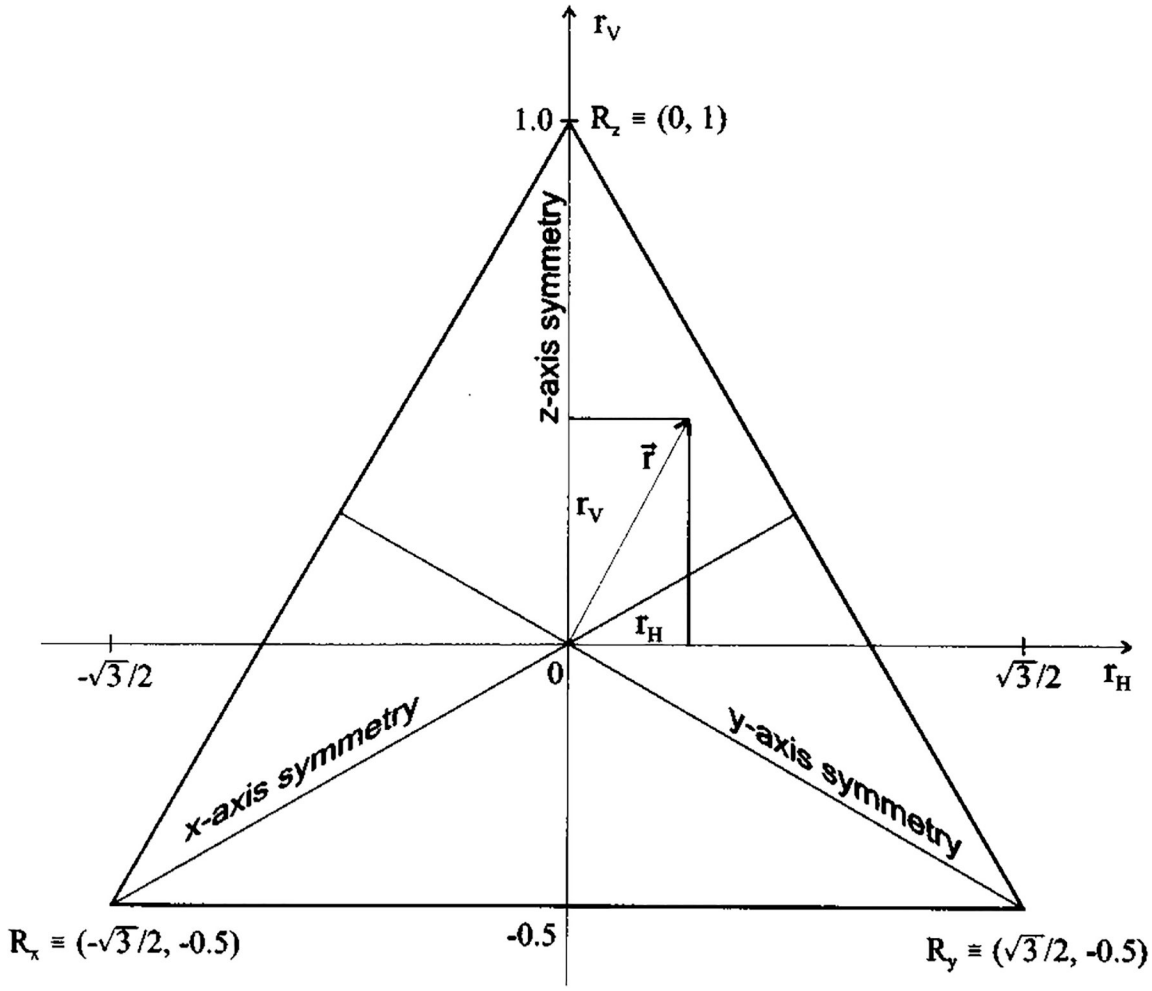

FIG. 4.

The triangle of anisotropy. All possible values of anisotropy are placed inside this triangle and are described by different values of the projections r_H and r_V of the anisotropy vector **r**. In the particular case of the *z*-axis cylindrical symmetry of the emission field r_H=0 and the anisotropy is described by magnitude of the projection r_V varying from −0.5 to +1.0.

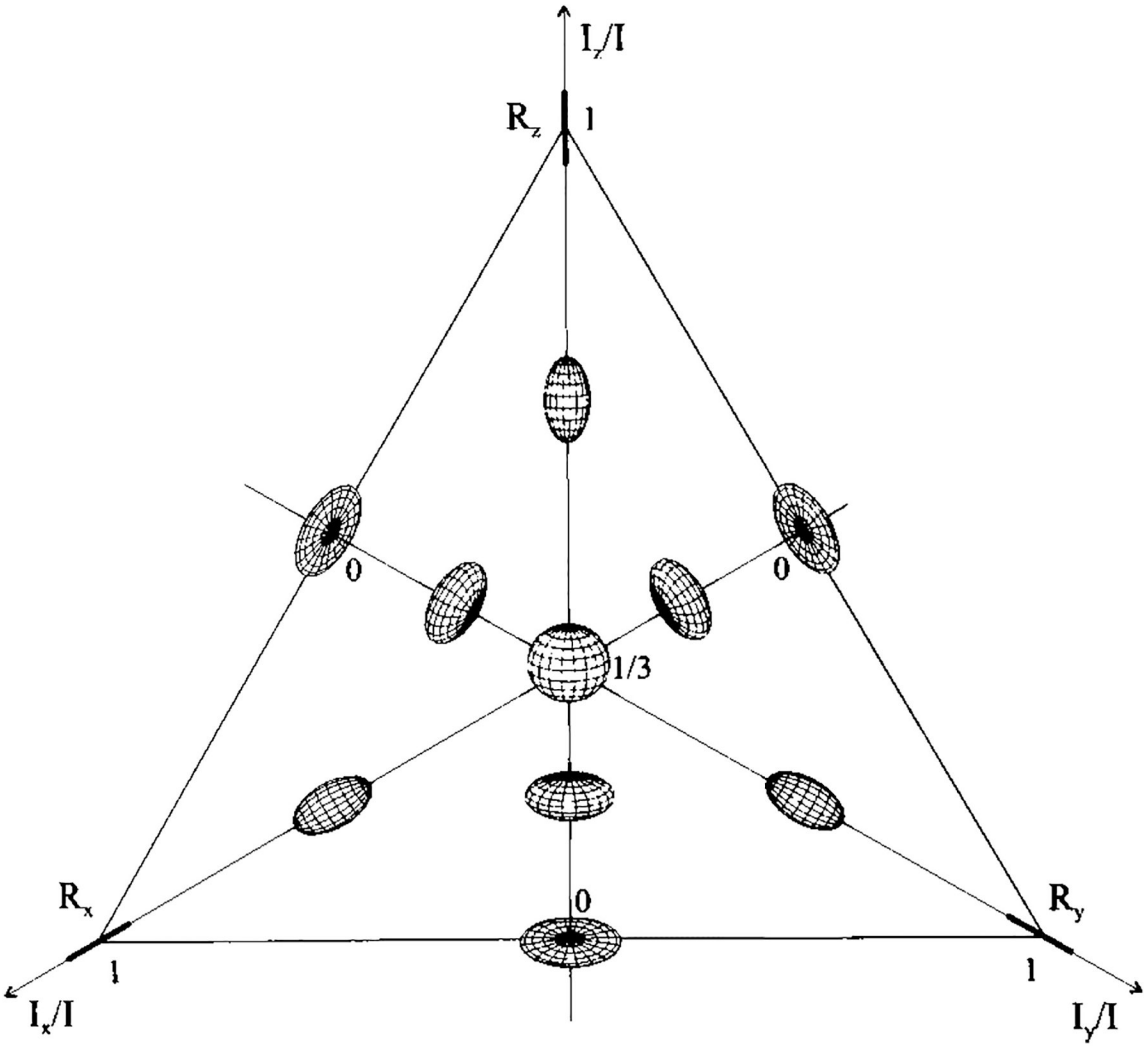

FIG. 5.

Approximate polar plots of the emission fields corresponding to the particular areas of the triangle of anisotropy. The relative intensities, I_X/I, I_Y/I, and I_Z/I, vary along the respective medians of the triangle from zero to unity. The centroid of the triangle corresponds to $I_X/I=I_Y/I=I_Z/I=1/3$ and to the spherically symmetrical emission field, whereas the vertices of the triangle correspond to the emission fields which are rodlike along the respective axes of the coordinate system (x,y,z).

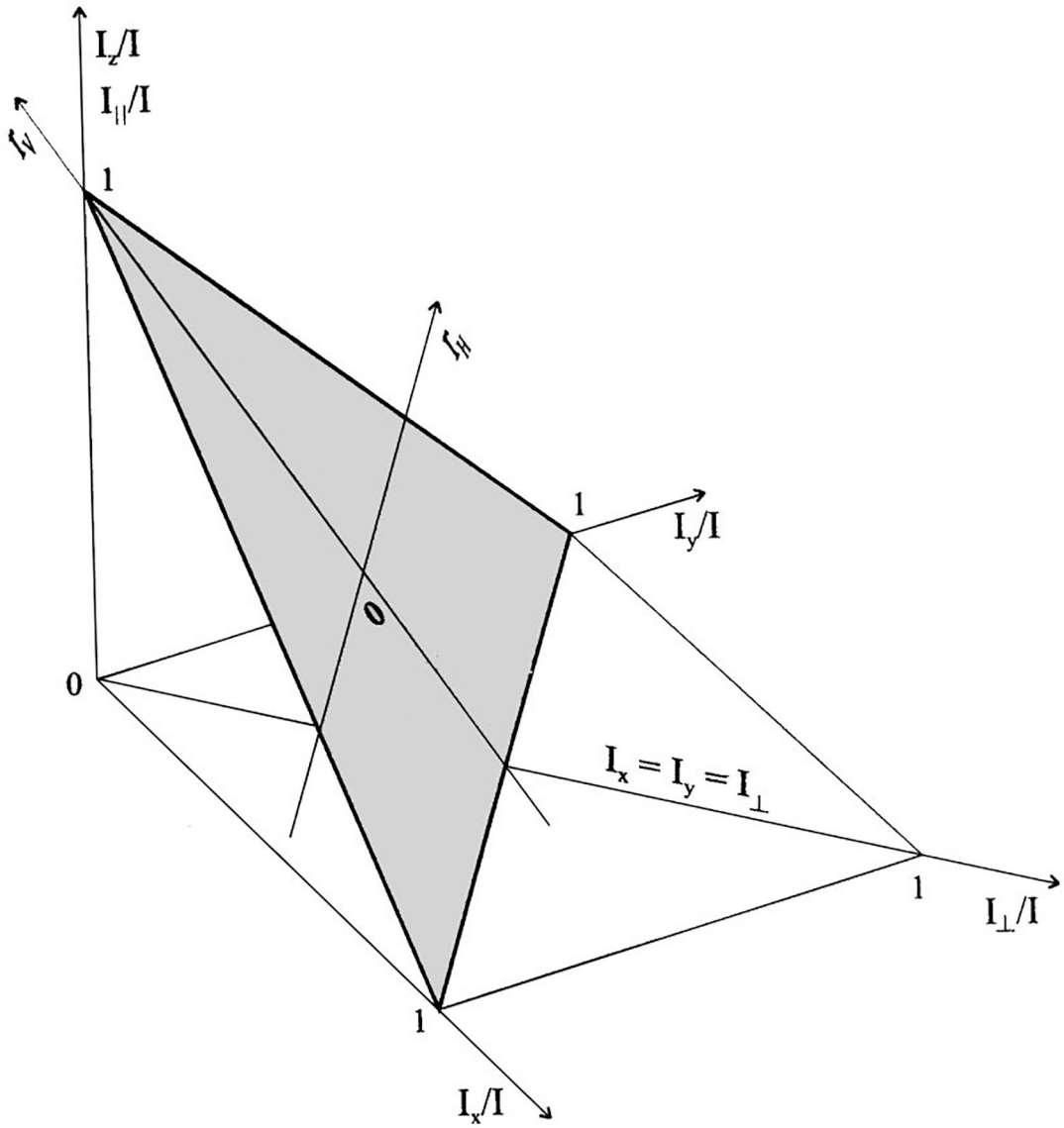

FIG. 6.

Position of the triangle of anisotropy and the coordinate system (r_H, r_V) in the coordinate system ($I_X/I, I_Y/I, I_Z/I$).

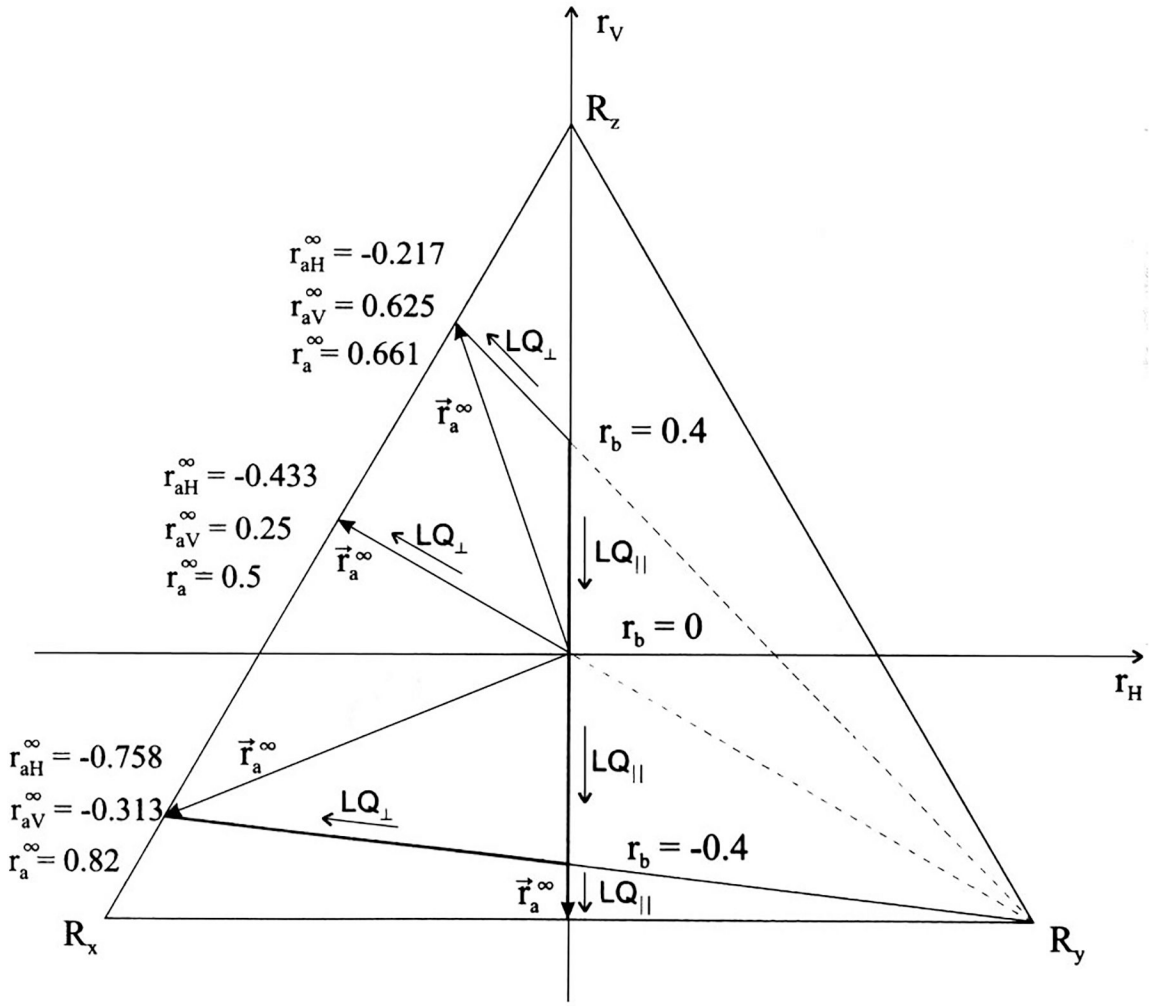

FIG. 7.

Possible changes of the anisotropy vector in parallel ($LQ_{\|}$) and perpendicular ($LQ_{\perp}$) light quenching for different values of the anisotropy r_b immediately before the arrival of the quenching pulse. In the parallel light quenching $\Delta r_H=0$ and $\Delta r_V\leqslant 0$. In the perpendicular light quenching $\Delta r_H\leqslant 0$ and $\Delta r_V\geqslant 0$. The short arrows show the direction of increasing power of the quenching pulse. The long arrows show the anisotropy vectors describing the respective emission fields after quenching by extremely intensive light pulses.

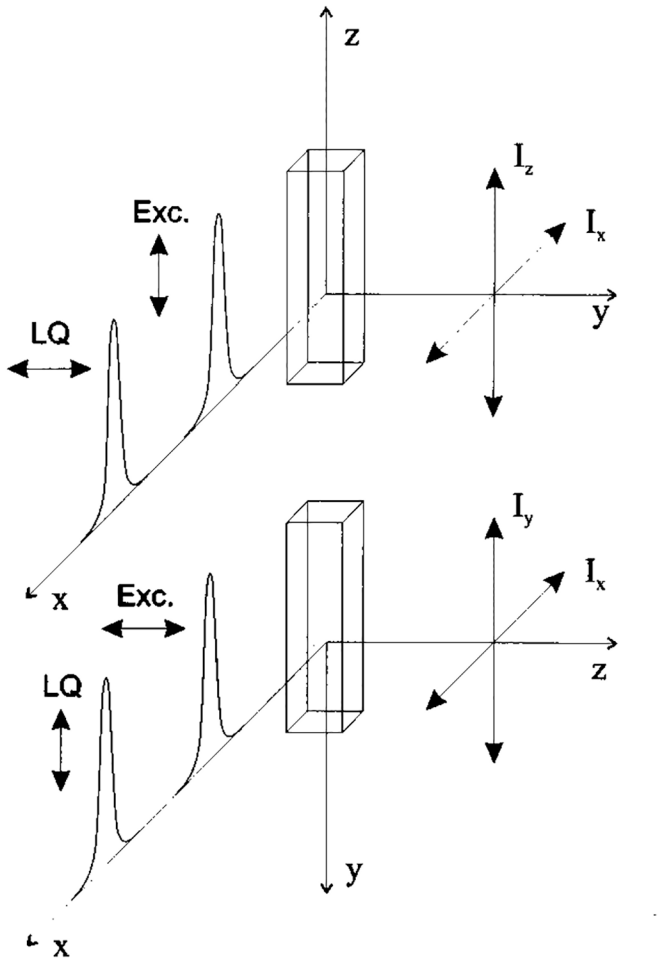

FIG. 8.

Illustration of the method of the registration of all three components of the polarized intensity with the same right-angle observation using vertical and horizontal polarization of the exciting beam.

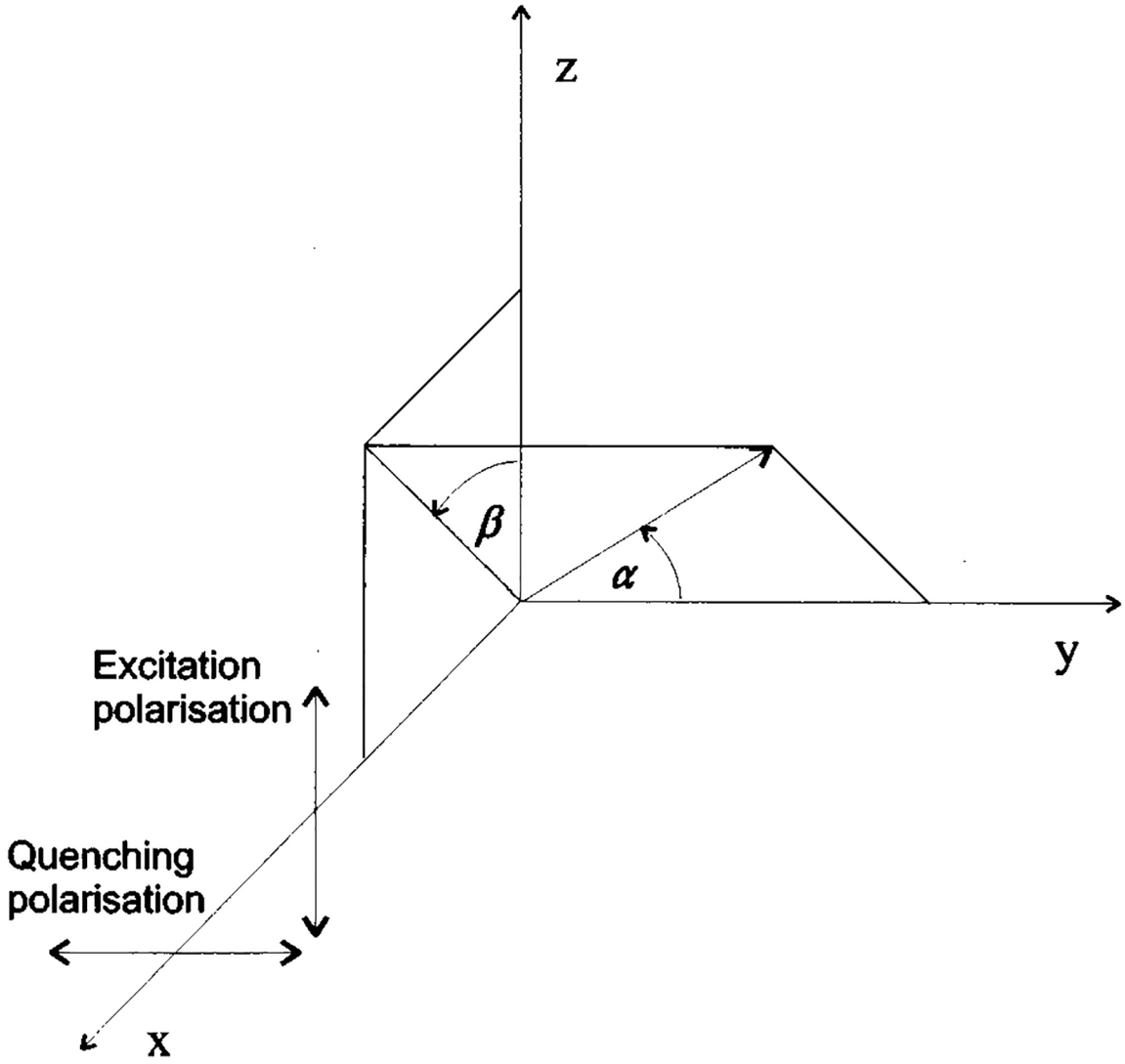

FIG. 9.

Spherical coordinate system used to prove that during the perpendicular light quenching experiments the polarized intensity ratio I_x / I_z remains unaffected.